

## How Antigen Quantity and Quality Determine T-Cell Decisions in Lymphoid Tissue<sup>▽†</sup>

Huan Zheng,<sup>1</sup> Bo Jin,<sup>1</sup> Sarah E. Henrickson,<sup>4</sup> Alan S. Perelson,<sup>5</sup>  
Ulrich H. von Andrian,<sup>4</sup> and Arup K. Chakraborty<sup>1,2,3\*</sup>

*Departments of Chemical Engineering,<sup>1</sup> Chemistry,<sup>2</sup> and Biological Engineering,<sup>3</sup> Massachusetts Institute of Technology,  
77 Massachusetts Avenue, Cambridge, Massachusetts 02139; Department of Pathology and Immune Disease Institute;  
Harvard Medical School, 77 Louis Pasteur Avenue, Boston, Massachusetts 02115<sup>4</sup>; and  
Theoretical Biology and Biophysics, Los Alamos National Laboratory,  
Los Alamos, New Mexico 87545<sup>5</sup>*

Received 24 January 2008/Returned for modification 10 February 2008/Accepted 4 April 2008

**T lymphocytes (T cells) express T-cell receptor (TCR) molecules on their surface that can recognize peptides (p) derived from antigenic proteins bound to products of the major histocompatibility complex (MHC) genes. The pMHC molecules are expressed on the surface of antigen-presenting cells, such as dendritic cells (DCs). T cells first encounter antigen on DCs in lymph nodes (LN). Intravital microscopy experiments show that upon entering the LN containing antigen, CD8<sup>+</sup> T cells first move rapidly. After a few hours, they stop and make extended contacts with DCs. The factors that determine when and how this transition occurs are not well understood. We report results from computer simulations that suggest that the duration of phase one is related to the low probability of productive interactions between T cells and DCs. This is demonstrated by our finding that the antigen dose and type determine when such a transition occurs. These results are in agreement with experimental observations. TCR-pMHC binding characteristics and the antigen dose determine the time required for a productive T-cell–DC encounter (resulting in sustained contact). We find that the ratio of this time scale and the half-life of the pMHC complex itself provide a consolidated measure of antigen quantity and type. Results obtained upon varying different measures of antigen quantity and type fall on one curve when graphed against this ratio of time scales. Thus, we provide a mechanism for how the effects of varying one set of parameters are influenced by other prevailing conditions. This understanding should help guide future experimentation.**

Recent multiphoton and confocal microscopy experiments have produced vivid images of the migration of T cells in lymphoid tissues during antigen recognition (2, 6–8, 11, 23, 30, 32–34, 37, 38, 40, 43, 47). For both CD4 and CD8 T cells, the motility characteristics change with time. Initially, T cells move quite rapidly upon entering the lymph node (LN). In the presence of cognate antigen, after a few hours, antigen-specific T cells slow down and make stable contacts with dendritic cells (DCs) presenting cognate antigen (6, 23, 30, 32, 33, 37, 38, 40). For CD8 T cells, these two stages of different T-cell motility have been labeled “phase one” and “phase two” behavior (30). It seems reasonable to assume that phase one corresponds to a period during which T cells “hunt” for antigen, whereas phase two is a period of time required for signaling processes that result in a full commitment to activation (30, 33). An important open question is which factors determine the time required for the transition from phase one to phase two. This is important, since this decision predicates T-cell activation and the initiation of an immune response.

Several hypotheses could be considered to address this ques-

tion. One is that T cells may go through such motility changes by default (30). This hypothesis implies that all antigen-specific T cells in the LN would transition into phase two synchronously and that the time at which this happens should be independent of the antigen dose or stimulatory potency. However, it seems more likely that this transition is linked to signaling events stimulated by interactions of T-cell receptor (TCR) molecules on the surfaces of T cells with cognate, peptide-loaded major histocompatibility complex (pMHC) molecules expressed on DCs. This suggests a second hypothesis: the transition from phase one to phase two is influenced by the nature of cognate pMHC ligands, their expression levels on DC surfaces, and the number of DCs in the LN that bear cognate antigen. In this case, the time at which a particular T cell transitions from phase-one- to phase-two-type behavior depends on its history of interactions with DCs, which are stochastic in nature but also have a relatively broad distribution over time. We also explored the consequences of summation of multiple interactions with antigen-presenting cells for the duration of phase one. We have studied how all of these variables collectively define the duration of phase one using computer simulations and theoretical calculations.

Migrating T cells stochastically encounter DCs bearing antigen which, in turn, can stimulate a stop signal with some probability, thereby leading to sustained contacts. We find that the average antigen dose per DC, the number of DCs bearing antigen, and the characteristics of the TCR-pMHC interaction

\* Corresponding author. Mailing address: Massachusetts Institute of Technology, Room E19-502C, 77 Massachusetts Avenue, Cambridge, MA 02139. Phone: (617) 253-3890. Fax: (617) 258-5766. E-mail: arupc@mit.edu.

† Supplemental material for this article may be found at <http://mcb.asm.org/>.

▽ Published ahead of print on 21 April 2008.

TABLE 1. Symbols used to represent important quantities

Symbol	Description	Unit(s)
$D$	Motility coefficient	$\mu\text{m}^2/\text{min}$
$k$	Probability of stop signal upon T-cell–DC encounter; depends upon TCR-pMHC binding characteristics and concn of antigenic pMHC per DC	$\text{min}^{-1}$
$p$	Concn of cognate-pMHC on DC surface	No./DC
$t$	Time	h
$\rho$	Density of cognate DCs in the LN	No./ $\mu\text{m}^3$
$\tau$	Characteristic time scale for peptide dissociation from MHC groove	h
$\tau_e$	Avg time for T cell to encounter cognate DC via motion characterized as random walk	h
$\tau_s$	Characteristic time required for productive T-cell–DC encounter; depends upon TCR-pMHC binding characteristics, no. of cognate DCs in LN, and pMHC concn on DC surface	h

determine the mean time required for a transition from phase one to phase two. Our results on how the antigen dose per DC and numbers of antigen-bearing DCs affect the duration of phase one are in excellent agreement with experimental observations described by Mempel et al. (30) and Henrickson et al. (22). Importantly, theoretical analyses of the computational and experimental results provide a conceptual framework for understanding how the effects of changing one measure of antigen dose or type on the duration of phase one depend on the values of other related quantities that also play a role in T-cell activation *in vivo*. We find that an interplay between two time scales which encapsulate the effects of antigen characteristics and amount is important. One of the time scales is the half-life of the pMHC complex, which characterizes its stability. The other time scale characterizes typically how long it takes for a productive T-cell–DC encounter to occur. Results for the duration of phase one obtained by varying diverse measures of antigen quantity and type collapse onto one consolidated “master” curve when antigen quality and type are measured by the ratio of these two time scales. The mechanistic principle embodied in this result should help guide future experimentation, because it shows how the effect of changing one variable is influenced by other relevant parameters.

#### MATERIALS AND METHODS

**Model and simulation method.** (i) **Model development.** Beltman et al. (4, 5) have studied T-cell migration in a realistic representation of the densely packed physical environment of the LN using a computational method based on the cellular Potts model. These simulations faithfully reproduce many experimentally observed quantities that characterize T-cell motility, such as velocity distributions, T-cell/DC scanning frequencies, etc. These studies also suggest that changes in velocity distributions observed upon transition to phase-two-type behavior require strong adhesion and stop signals from cognate DCs. Quantitative recapitulation of the experimental and computational facts regarding T-cell motility (e.g., velocity distributions) is not the purpose of our *in silico* studies. While our investigations are closely synergistic with experiments (22), our purpose is to glean qualitative mechanistic principles that determine the duration of phase one. Specifically, we aimed to elucidate how variables such as the cognate pMHC dose per DC, the number of cognate DCs, the stability of pMHC, etc., influence this duration (Table 1). This goal guided the choice of the model that we simulated and analyzed.

We use a lattice representation of the space corresponding to the LN (Fig. 1) with periodic boundary conditions in which the edges of the box (e.g., left and right or top and bottom) are essentially pasted together. Thus, for example, when a cell exits the box on the left, it reappears on the right. This enables simulation of the large spatial extent of the LN ( $\sim 1 \text{ mm}^3$ ) with no collisions of T cells with the faces of the simulation box. Each type of cell (e.g., a T cell or a DC) can occupy one of the lattice sites. Motile cells can hop from one lattice site to a neighboring one. This discrete, rather than continuous, representation of space dramatically reduces the computational power required to simulate the effects of

specific parameters characterizing the antigen dose and type on the duration of phase one. The lattice representation does not lead to artifacts as long as the properties of interest are manifested on long time and length scales (16) (and one other condition noted later is met). As we focus on the transition from phase-one to phase-two behavior, which occurs on a time scale that far exceeds the microscopic time associated with cell motion between lattice sites and signaling events during transient T-cell–DC encounters, a lattice representation is appropriate. We also note that while our stochastic simulations allow us to examine the important effects of fluctuations, the average values of the simulation results agree with those obtained from a mean field treatment that does not use a lattice representation. Therefore, for the qualitative results that we seek, the lattice representation seems adequate.

The lattice is 30 by 30 by 30 units in size. Only antigen-specific T cells were explicitly simulated to obtain the results shown here. Simulations wherein noncognate T cells were included showed that the results were affected only when there were vastly many noncognate T cells; at lower levels the results are unaffected by their presence (Table 2).

The T cells can be either motile or arrested. Intravital microscopy data suggest that T cells move in a directed fashion over distances of the order of  $10 \mu\text{m}$  before changing direction randomly (3, 7, 30, 32–34). On large length and time scales, the statistical features of the motion are those characteristic of a random walk. Experiments also show that the average speed of migrating T cells is on the order of  $10 \mu\text{m}/\text{min}$ . In view of these facts, we consider the spacing between points on the lattice to be  $10 \mu\text{m}$  and the elementary time step to be 1 min. This means that our simulation box is approximately  $300 \mu\text{m}$  by  $300 \mu\text{m}$  by  $300 \mu\text{m}$  in size. Our simulation results apply also to other choices of the average directional movement (e.g.,  $20 \mu\text{m}$ ), because such changes would require a simple rescaling of the lattice dimension ( $20 \mu\text{m}$  instead of  $10 \mu\text{m}$ ). The simulation period of 1,440 elementary steps corresponds to a 24-h residence period of T cells in the

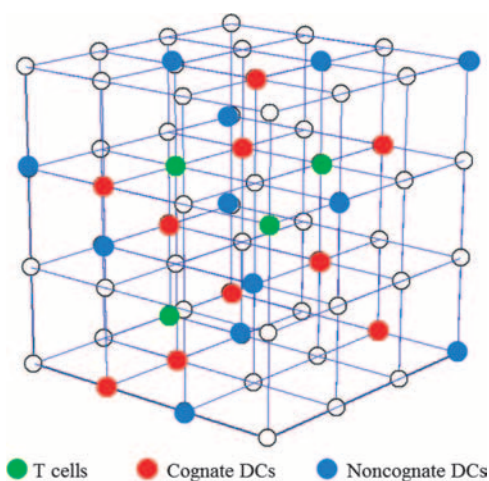


FIG. 1. Lattice representation of the volume in the LN that is subject to computer simulations. Cognate and noncognate DCs and T cells are shown schematically.

TABLE 2. Parameters associated with simulation<sup>a</sup>

Parameter	Variation	Effect(s)	Brief justification
p, cognate DCs	100 to 800	Larger p, shorter phase one, lower threshold [pMHC]	Larger p, more frequent T-cell-DC encounters, more activation attempts early on when [pMHC] has not yet decayed much
Cognate T cells	250, 500, 750	Virtually no difference	Fractional occupation of lattice by cognate T cells is very low; collisions are not likely
Noncognate T cells	0 to 15,000	Virtually no difference at low loading (<5,000). Then more non-cognate T cells, higher threshold [pMHC]	Very high loading of noncognate T cells causes "jamming" in the lattice (see Methods)
p-k mapping	Threshold location and sharpness (see Fig. 2)	Sharper or lower threshold both reduce the threshold [pMHC] required for phase two	Both lead to slightly higher stoppage probability k at the same initial [pMHC]
Scanning time	1, 3, 5 min	Longer scanning time, shorter phase one, faster transition to phase two	Longer scanning, more attempts to stop T cell, thus increasing the probability of a stop signal
Activation scheme	Main scheme in the text; alternatives as described in legend for Fig. 4	(i) No difference between main scheme and alternative 3; (ii) alternative 2 has only slightly lower arrest fraction	(i) k change due to peptide dissociation during the short waiting is insignificant; (ii) only 1 attempt to stop T cell reduces stoppage probability
Exit time, $T_e$	10 to 27 h	Virtually no difference	Important time scales are all much shorter than exit time
Stability of pMHC complex, $\tau$	100 to 800 min	More-stable pMHC requires lower threshold [pMHC] to transition to phase two	Slower dissociation of pMHC, slower decline of k
Time scale of memory decay, $\tau_m$	0 to 250 min	Larger $\tau_m$ reduces threshold [pMHC] to some maximum extent	Effectively increasing k by compounding remnant k from previous encounters

<sup>a</sup> Various parameters associated with the simulation, and components of the simulation scheme, were varied to examine the robustness of our results. In all cases, the qualitative behaviors remain unchanged. The variations are listed here, along with their main quantitative effects, if any. A brief explanation is provided for each variation to rationalize the relevant quantitative differences in the results.

LN (21). This simulation period is chosen because if T cells do not get activated and upregulate CD69 (39), they migrate out of the LN after approximately 24 h (21).

We consider two types of DCs, those bearing cognate pMHC ligands (cognate DCs) and those that do not display these molecules. Since intravital multiphoton microscopy results have shown that DCs are far less motile than T cells (7, 8, 32), in all our simulations the DCs are immobile. This will not affect qualitative results, because the motion of DCs simply affects the frequency of T-cell-DC encounters. It can be rigorously proven that in a system where the DCs are immobile, the T-cell-DC encounter frequency equals that where they are allowed to move if the motility coefficient characterizing T-cell motion is taken to be the sum of that for T cells and DCs. As we discuss later, the encounter frequency does not limit the transition from phase-one to phase-two behavior, and thus, accounting for the slow movement of DCs is not important for the issues we study. Therefore, different choices and/or random distributions of T-cell speeds (e.g., centered around 10  $\mu\text{m}/\text{min}$ ) will also not have an important effect.

A larger number of noncognate DCs create more barriers for T-cell migration, resulting in a lower T-cell motility coefficient. Thus, we adjusted the number of noncognate DCs to obtain a motility coefficient consistent with the experimentally measured values (30, 32, 33). A motility coefficient of 11  $\mu\text{m}^2/\text{min}$  was obtained with 3,000 noncognate DCs placed in the lattice. The numbers of cognate DCs and T cells span a range of values (from 100 to 1,000 for DCs and from 250 to 750 for T cells) in our simulations in order to examine their effects on the time at which a transition from phase-one to phase-two behavior occurs.

Henrickson et al. measured that a typical LN imaged in the experiments is approximately 1  $\text{mm}^3$  in volume, of which roughly 5 to 10% is the volume where relevant migration takes place. They also estimated that 300 cognate DCs are scattered therein, resulting in a density of 3,000 to 6,000 cognate DCs per 1  $\text{mm}^3$ . Since our entire lattice is scaled to be 0.027  $\text{mm}^3$ , the appropriate number of cognate DCs in the lattice should be on the order of 100 cells. Most of our simulations have been carried out with 100 cognate DCs and 500 cognate T cells, and qualitative results do not change upon varying these cell counts (Table 2).

We have carried out simulations wherein the total numbers of DCs and T cells occupy as much as 50% of the available volume, which is lower than the fraction of space occupied by cells in a normal LN (10, 50). Simulations with higher

densities of cells become computationally intensive. If we explicitly simulated all the noncognate DCs and T cells, the following artifact of the lattice representation (which makes the simulations computationally tractable) would render the results less meaningful. Since we model T cells as hard objects that cannot occupy sites already inhabited by other T cells, including a very large number of noncognate T cells and DCs would lead to a "jamming" of the lattice, in which case no cell would move. In reality, of course, space is continuous and T cells are deformable, and so such a jamming does not occur in the LN. Our goal is to determine qualitative mechanisms via which T-cell motility is influenced by cognate pMHC. These qualitative mechanisms should not be affected by using fewer cells so that the jamming artifact is not manifested.

At the beginning of a simulation, all cells are placed randomly on the lattice and all T cells are motile. T-cell motion is simulated using a Monte-Carlo algorithm (see "Simulation method"). In short, a T cell is picked randomly, and an attempt is made to displace it in a random direction. If the chosen target site on the lattice is not occupied by another T cell, then the T cell moves to the new location. T cells are allowed to occupy the same site as a DC because they have been observed to sit on the surfaces of DCs and scan for antigen (7, 23, 30, 32, 33, 38, 40, 43). In addition, DCs have been observed to extend out multiple dendrites from their center of mass, and these protrusions are longer than 10  $\mu\text{m}$  (30, 32). Since a DC can interact simultaneously with several T cells and encounters between DCs and T cells can occur simultaneously at several dendrites (7, 30, 32, 33), in our model, T cells at the six lattice points surrounding a DC can simultaneously interact with it and scan for antigen. Along with the fact that T cells can cooccupy the same lattice point as a DC, in principle, a large number of T cells (exceeding six) are allowed to scan a DC simultaneously, as observed in experiments. Experiments have also shown that the brief contacts during phase one last for about 3 min (7, 20, 30, 32–34), which we model by introducing a scanning time equal to three Monte-Carlo steps (this corresponds to approximately 3 min). T cells that encounter a DC do not move until this scanning time period has elapsed. Varying the length of scanning time does not alter the results qualitatively (Table 2).

During the scanning period, interactions between the TCR and pMHC on DCs, as well as integrins, costimulatory molecules, and cytokines, result in intracellular signaling events that could lead to a stop signal (24). It remains an

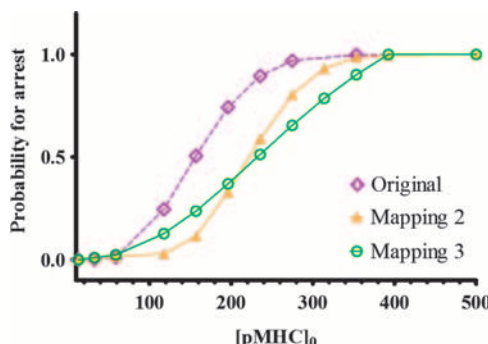


FIG. 2. Probability for T cells to receive a stop signal upon encountering a cognate DC ( $k$ ) plotted against the concentration of pMHC on DCs after pulsing with peptide prior to adoptive transfer. Original mapping (green circles) corresponds to the mapping used for the results presented in the text, as described in Materials and Methods. To demonstrate how such mapping can be varied, two alternatives are shown. Alternative 1 (orange triangles) is a mapping with the pMHC threshold moved to the right (i.e., a higher initial loading of pMHC is needed for the same probability of stopping), while alternative 2 (purple circles, dotted line) maintains the original threshold location but exhibits a sharper response. As a consequence,  $k$  increases more sharply as the initial pMHC concentration is increased.

open question whether T cells can integrate signals from multiple serial encounters with cognate DCs (11, 15, 20, 40) or a threshold level of signaling must result from encounters with a single DC (14, 23, 25, 31, 45, 46). We consider both scenarios, one in which T cells can integrate signals from serial encounters with DCs and the other, in which any signaling resulted from a T-cell-cognate DC encounter is “forgotten” instantly after the T cell disengages.

In the latter situation, if a T cell encounters a cognate DC, signaling can lead to a stop signal with a probability equal to  $k$  (implemented as part of the Monte-Carlo algorithm described below). This probability is related to the characteristics of the TCR-pMHC interaction and the level of pMHC expression on the surface of the DC. Our model for T-cell migration must be linked to molecular signaling models (e.g., see references (1, 12, 18, 28, 29, and 49) in order to properly link  $k$  to these quantities which reflect antigen quality and quantity. While such a sophisticated multiscale model is under development, in the present study we adopt a simpler approach. We model the relationship between  $k$  and the antigen concentration with a sigmoidal curve which exhibits a threshold antigen concentration above which  $k$  is large and below which  $k$  is small (Fig. 2). This shape is chosen because experimental results for markers of T-cell signaling/activation exhibit such dose-response curves (e.g., see references 29 and 44)). The value of  $k$  is zero when the antigen concentration is zero and approaches one for large values of the antigen dose. A function with a sigmoidal shape was used to interpolate values of  $k$  between these asymptotes (see “Simulation method”). Different TCR-pMHC binding characteristics alter the threshold concentration defined by the sigmoidal curve and its sharpness. While the results in the main text are for a particular choice of the location and sharpness of the threshold of this sigmoidal curve, we found that changing the values of these variables only results in quantitative, rather than qualitative, differences (Table 2).

To study situations where T cells can integrate signals from multiple DCs, the probability of generating a stop signal ( $k$ ) upon a particular T-cell-DC encounter is modeled to depend upon the history (or experiences) of that particular T cell as it migrates through the LN. The specific way in which  $k$  depends on history in our simulations is described in the context of our results.

Most intravital microscopy experiments are conducted several hours after antigen (peptides targeted to DCs, protein and adjuvant injected subcutaneously, or adoptively transferred antigen-pulsed DCs) is injected into mice (2, 6–8, 23, 30, 32–34, 37, 38, 40, 43, 47), and the transition from phase-one- to phase-two-type behavior can occur several hours after T cells enter the LN (30, 33, 40). Thus, an important variable is the time scale over which cognate peptides are lost from MHC molecules. As we shall see, this variable can have an important effect on the time corresponding to a transition from phase one to phase two. This effect is studied in the computer simulations by varying the characteristic time scale,  $\tau$ , which describes the first-order dissociation process via which the antigen concentration on DCs decreases over time.

(ii) **Simulation method.** For each Monte-Carlo move (17), a random integer drawn from a uniform distribution of integers from 1 to  $N$  (where  $N$  is the number of T cells) is used to pick a T cell, and an attempt is made to displace it to a neighboring lattice point in a randomly chosen direction. If the chosen T-cell has not yet received a stop signal and the proposed location is not occupied by another T cell, the T cell moves to the new location. Otherwise, the move is rejected and the T cell stays in place.

A T-cell-DC encounter occurs when a T cell either moves to a lattice point directly occupied by a DC or is at the site immediately adjacent a DC site. When a T cell encounters a DC, it waits (and scans for antigen) for three time steps (other values were tested, as shown in Table 2). When a T cell contacts a cognate DC, it can receive a stop signal with some time-dependent probability,  $k(t)$  (see above). In the case without memory,  $k(t)$  is calculated using the pMHC concentration of the DC,  $p(t)$ , with which the T cell is currently interacting. Following experimental observations (29, 44),  $k(t)$  is related to  $p(t)$ , using the sigmoidal function shown below:

$$k(t) = \begin{cases} 4 \times 10^{-3} p(t), & p(t) \leq 3 \\ \frac{1.2218p(t)^2 - 1.9878p(t)}{734.118 - 19.7905p(t) + p(t)^2}, & 3 < p(t) < 30 \\ 1, & p(t) \geq 30 \end{cases} \quad (1)$$

Note that in the above expressions, the time,  $t$ , refers to the time after the DCs have arrived in the LN, which is also the time for the T-cell transfer and is approximately 18 h after pulsing DCs with peptides and injection into animals in the experimental studies of Henrickson et al. (22). To trace back to the initial pMHC loading on DC surfaces,  $[pMHC]_0$ , one needs to account for the loss of peptides during the 18 h, which can be estimated as  $[pMHC]_0 = p(0)\exp(-18/\tau)$ , where  $\tau$  is the time scale of pMHC loss in units of hours, and we have used values for  $\tau$  reported in the legend of Fig. 3. Changing the values of the constants in equation 1 represents changing the TCR-pMHC binding characteristics since it alters the threshold antigen dose and sharpness of the relationship between  $k$  and the antigen dose. We also performed simulations with either the threshold location or the sharpness altered (see Results and Table 2 for details).

In the case without memory, at the beginning of each elementary time step,  $p(t)$  and  $k(t)$  are updated. When a T-cell-cognate DC encounter occurs, a uniform random number ( $r$ ) between 0 and 1 is generated and compared with the current value of  $k(t)$ . If  $r < k$ , the T cell receives a stop signal. If  $r \geq k$ , the T cell waits one step and repeats the activation attempt in the next step, with the same value of  $k$  as in the previous step. This procedure is chosen because we imagine that pMHC loss from the T-cell-DC contact zone is unlikely. If no arrest has occurred after three steps have elapsed, the T cell starts migrating again. T cells in contact with noncognate DCs cannot receive a stop signal. We have also examined the case in which peptide loss is allowed in the contact zone, as well as the scenario where it is only possible to deliver a stop signal during the first scanning step. In both cases, the qualitative results (Table 2) do not change.

This simulation protocol is modified slightly to incorporate signal integration, i.e., the “memory” effect. The details will be discussed in the next section along with relevant results.

## RESULTS

We have considered situations where T cells can and cannot integrate signals from serial encounters with DCs. We begin by reporting results from simulations and theoretical calculations where naive, recirculating T cells do not exhibit a “memory” of past encounters with cognate antigen-bearing DCs in the LN.

**Phase-one-to-phase-two transition is determined by antigen quality and quantity.** In our simulations, antigen quality and quantity are determined by three variables: (i) the initial concentration of cognate pMHC ligands on the DC surface and their TCR binding characteristics, which determines the probability ( $k$ ) that a particular T-cell-cognate DC encounter will result in a stop signal; (ii) the stability of complexes formed between the cognate peptide and MHC proteins; and (iii) the density (or number) of DCs in lymphoid tissue that present these ligands.

The amount of cognate pMHC on DC surfaces, and hence the value of  $k$ , changes with time as peptides dissociate from the

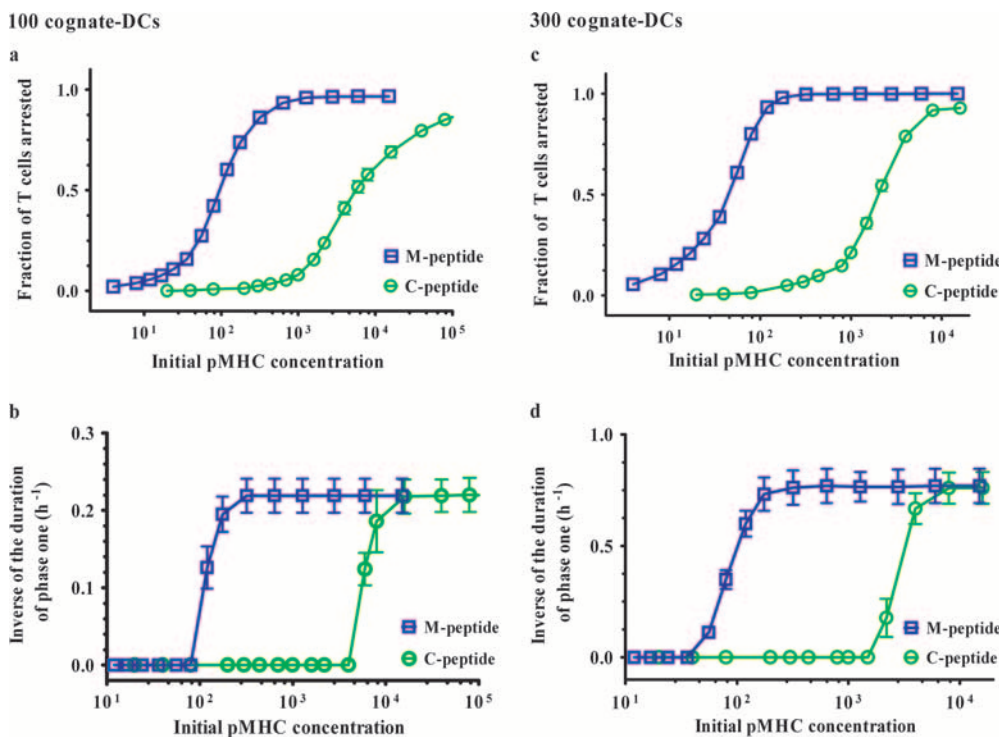


**FIG. 3.** Antigen dose and type determine the transition from phase-one- to phase-two-type behavior. Computer simulation results for the fraction of T cells that have been arrested before the exit time has elapsed (a and c) and the inverse of the mean duration of phase one (b and d) as a function of the concentration of pMHC on DCs prior to adoptive transfer into recipients. The duration of phase one is defined as the time required for 50% of the T cells to make sustained contacts with DCs, as described in the text. The relationship between the units of concentration on the abscissa of the graphs and the concentrations of peptides used to pulse DCs in experiments carried out by Henrickson et al. (22) is described in the text. If a transition to phase two does not occur prior to exit, the duration of phase one is taken to be infinite, in which case the inverse of the duration of phase one is zero, as seen in panels b and d. Results for two pMHC ligands, characterized by different half-lives of the pMHC complex, are shown. The values of the half-life that were used are approximately 6 h and 2.35 h, since that roughly corresponds to the experimentally determined pMHC half-lives for the M peptide and C peptide, respectively (22). These peptides are the natural (C) and an altered (M) peptide ligand for the P14 TCR transgenic system. One hundred cognate DCs (a and b) or 300 cognate DCs (c and d) are analyzed.

MHC groove. The stability of the pMHC complex is described by the parameter  $\tau$ , which is the time associated with peptide dissociation from the pMHC complex. This parameter, along with the initial concentration of antigen loaded onto DCs before adoptive transfer, determines the antigen concentration displayed on DC surfaces at any given time. The density (related simply to the number) of cognate DCs in the LN is described by a single parameter ( $\rho$ ).

Figure 3a and c show that the fraction of T cells arrested before the exit time (24 h) has elapsed depends on antigen quality and quantity. The fraction of T cells arrested increases as the initial antigen loading and the density of cognate DCs are increased. This is because a higher density of cognate DCs (e.g., 300 versus 100 cognate DCs per lattice) increases the probability of a T-cell–cognate DC encounter, while a higher antigen concentration on DCs corresponds to a higher probability for the T cell to receive a stop signal (i.e., higher  $k$ ). Varying the exit time between 10 and 27 h led to barely any change in the results (see Table 2 for a discussion). Note also that since the arrested cells are the ones most likely to commit to full activation (24), late activation markers (e.g., proliferation) likely change in ways that parallel the changes in the fraction of arrested cells; thus, the fraction of arrested cells can be considered to be a measure of late markers of activation.

The results displayed in Fig. 3b and d make direct the connection with the experimental observations of Henrickson et al. (22), who observed the T-cell migration patterns in LNs containing adoptively transferred DCs pulsed with various antigenic peptides ex vivo. Henrickson et al. define the time corresponding to the transition from phase one to phase two as that at which some large fraction (e.g., 50% of the T cells) is no longer motile (i.e., the median times of interaction between antigen-specific T cells and peptide-pulsed DCs are greater than 30 min in a 60-min observation period). T cells do not transition to phase two in a synchronous manner. The duration of phase-one-type behavior for individual T cells in each of our in silico trajectories varies widely (from minutes to hours), especially at the threshold concentration of pMHCs required to induce a transition to phase two. In experiments too, different T cells stop at different times. Similarly, because of the stochastic nature of this process, the duration of phase one observed by Henrickson et al. also differs from one experimental realization to another, fluctuating around some average value. Similar behavior is also captured in our simulations (see the supplemental material). In both our simulations and the experiments, an average value of the time at which a large fraction of T cells is arrested is reported. This time is repre-

sentative of the behavior of the population of T cells, but does not imply synchronous behavior for every T cell.

Figure 3b and d show how the average time at which 50% of the T cells are arrested depends on the initial value of the antigen concentration on DC surfaces and the density of cognate DCs (e.g., 300 versus 100 cognate DCs per LN). The shape of these curves is strikingly similar to that reported by Henrickson et al. for the dependence of the time of a transition from phase one to phase two on the peptide concentration used to pulse DCs ex vivo. Besides the two values of DC loadings displayed in Fig. 3, several other values were also tested and led to no qualitative difference (see the discussion in Table 2).

One of the pMHC ligands studied by Henrickson et al. (22) is called the “M peptide.” This is an altered peptide ligand for the P14 TCR transgenic system, wherein T cells recognize a peptide from lymphohochoriomeningitis virus (KAVYNFATC is the natural peptide, referred to as the C peptide, and KAVYN FATM is the “M peptide”). They report that for DCs pulsed with 100 pM of M peptide, a transition to phase two was not observed. Pulsing concentrations of 200 pM resulted in phase-two-type behavior after 6 to 8 h, and all higher pulsing concentrations led to a phase one that lasted 2 to 4 h (22). Thus, these experimental data seem to exhibit the thresholding (with 200 pM as the threshold) and asymptotic behavior observed in our simulation results. The thresholding behavior results from the nature of the dose-response curve characterizing T-cell signaling (Fig. 2).

The stability of pMHC determines the amount of cognate pMHC left on the DC surface at various times after adoptive transfer. Consequently, the time scale  $\tau$  characterizing pMHC dissociation influences T-cell migration and activation by affecting how the probability of productive signaling ( $k$ ) varies over time. Two values of  $\tau$  differing approximately by a factor of 2 (3.4 and 8.7 h, respectively) are considered in Fig. 3. These values were chosen because they correspond to the stability characteristics of the M and C peptides in the experimental studies of Henrickson et al. (22). We also explored a range of  $\tau$  values between 100 and 800 min; the qualitative behavior parallels those shown in Fig. 3 (see the discussion in Table 2). Our results show that while keeping all other parameters the same, values of  $\tau$  that differ by a factor of 2 can result in a substantial difference in the fraction of T cells arrested before the exit time has elapsed (Fig. 3a and c). Equivalently, the less-stable peptide requires a longer time to transition into phase two. Ligand concentrations that result in a transition to phase two for the M peptide would not lead to such a transition for the C peptide, as observed in experiments (22).

However, there are some subtleties. For example, at the threshold concentration required to observe a transition to phase two, the duration of phase one obtained from simulations is roughly the same for the M and C peptides (note, however, that this threshold concentration is much higher for the C peptide) if the TCR binds both pMHCs with the same affinity. In reality, however, the C peptide could bind TCR slightly more weakly than the M peptide. This can be modeled by moving the threshold in the relationship between  $k$  and the antigen concentration to higher concentrations. We could establish that while such changes do not alter our conclusions in qualitative ways, the results do change quantitatively (see the

discussion in Table 2). For example, shifting this threshold by a factor of 1.5 results in transition times around 9 h (ranging from 6 to 12 h) for the C peptide, which is consistent with experimental observations (22).

The results shown in Fig. 3 and corresponding experimental observations (22) show that antigen quality and quantity determine the duration of phase one.

**A consolidated measure of antigen quality and quantity determines the duration of phase one.** A common conceptual framework which reveals how antigen dose and type influence the duration of phase one is obtained by recognizing that the pertinent stochastic processes are described by distinct average time scales.

One potentially important time scale is the length of time required for T cells to encounter cognate DCs by effectively random processes. This time,  $\tau_e$  (the subscript “ $e$ ” denotes “encounter”), scales as  $1/(\rho^{2/3}D)$ , where  $\rho$  is the density of cognate DCs in the LN and  $D$  is the T-cell motility coefficient which is calculated from experimental results (30, 32–34). Experimental values of  $D$ ,  $\rho$ , and the duration of phase one make clear that  $\tau_e$  is much smaller than the duration of phase one. In other words, prior to exiting the LN, T cells have ample opportunities to encounter cognate DCs. This is consistent with Bousso and Robey’s findings that DCs scan at least 500 T cells per hour in the absence of antigen (7) and findings of other previous studies (5, 10, 32, 41). Similarly, our simulations are carried out for a range of conditions wherein  $\tau_e$  (the time required to encounter DCs) is not limiting.

Since different peptides are lost from the DC surface at different rates over time, another time scale, the characteristic time for peptide loss ( $\tau$ ) discussed earlier, is an important measure of the quality of an antigen. However, how different values of  $\tau$  affect the duration of phase one will depend on other key variables. For example, if the half-life of the pMHC complex is shorter (smaller  $\tau$  and less-stable pMHC), the effect on the duration of phase one will depend on the prevailing antigen dose. This is because a higher antigen dose could compensate for a less-stable pMHC. How do we properly compare the effect of a change in the antigen dose (units of molarity) with a change in the peptide half-life (units of time)? A systematic method to compare the relative impact of changing different measures of antigen quantity and type (each measured in different units) would be extremely useful for interpreting and designing experiments.

Assessing the impact of changing the value of one variable while taking into account the context (values of other pertinent variables measured in different units) is facilitated by grouping (e.g., as products or ratios) the relevant variables to obtain nondimensional quantities (13). The change in the value of such a nondimensional quantity upon altering a particular variable properly reflects the relative effect of manipulating this variable. Our goal is to compare the effect of a change in the stability of the pMHC (a time scale) with changes in other measures of antigen type and dose, such as TCR-pMHC binding characteristics, pMHC dose, and number of cognate DCs. To do this, we need to relate measures of these last quantities to a time scale pertinent to the process of T-cell–DC interaction.

As T cells migrate through the LN, the number of encounters with DCs (or time) required to receive a stop signal should

depend on the number of cognate DCs and pMHCs per DC and the TCR-pMHC binding characteristics (represented by the pMHC-to- $k$  mapping in our model). For example, small values of antigen concentration, cognate DC number, or half-life of the TCR-pMHC interaction will result in a longer phase one. In other words, the time required to receive a stop signal ( $\tau_s$ ) is determined by  $k$  and  $\rho$  (the number of cognate DCs in the LN). Thus, the effect of changing  $k$  or  $\rho$  is contained in one single variable: the time scale  $\tau_s$ .

The nondimensional grouping  $\tau/\tau_s$  allows an “apples to apples” comparison of the effects of antigen dose and TCR-pMHC binding characteristics with the half-life of the pMHC complex. If this hypothesis is correct, data obtained from varying diverse measures of antigen quantity and quality should collapse onto one consolidated master curve if graphed against the  $\tau/\tau_s$  ratio. How can the value of this ratio be obtained in terms of the individual measures of antigen quantity and quality?

Our computer simulations naturally include stochastic fluctuations which are normal for all biological systems. Stochastic effects can be important for many phenomena in molecular immunology (e.g., see references 29 and 49). The importance of stochastic effects for the transition from phase-one- to phase-two-type behavior is highlighted by the fact that for identical conditions, in our computer simulations the duration of phase one varies widely (over a range of 2 to 3 h) from one simulation to another. Experiments also show similar variability (22). This is not surprising, since for a related problem in physics (survival probability of particles diffusing in a medium composed of randomly placed sites that can trap the particles with some probability), the importance of stochastic fluctuations has been proven in a mathematically rigorous manner (26, 27). Also, the importance of stochastic effects has been noted by Preston et al. (35) in the context of T-cell migration in lymphoid tissue. Therefore, a computational treatment that *a priori* assumes that every T cell undergoes a transition from phase-one- to phase-two-type behavior at precisely the same time (the average value of the duration of phase one) is oversimplified. However, such a mathematical description can be useful in identifying how quantities (such as our time scale ratio  $\tau/\tau_s$ ) depend upon other parameters and may be satisfactory for obtaining the mean values of certain quantities.

In such a treatment, one writes down a differential equation for the spatiotemporal evolution of the concentration of the T cells that have not received a stop signal (denoted  $T$ ):

$$\frac{\partial T}{\partial t} = D\nabla^2 T - kpT \quad (2)$$

$$T(t = 0) = T_0 \quad T(t, \pm \infty) = 0$$

The spatially averaged solution has the form  $T/T_0 = \exp\{-\rho \int_0^t k(t')dt'\}$ . In other words, the number of T cells that have received a stop signal depends only on  $\rho \int_0^t k(t')dt'$ , which equals  $\tau/\tau_s$ .

We have carried out computer simulations wherein diverse measures of antigen quantity and quality are varied to examine whether all the resulting data collapse onto one consolidated

master curve when graphed against  $\tau/\tau_s$  (given by the last formula).

Figure 4 shows that all our simulation results (varying the initial antigen concentration, half-life of the pMHC complex, fraction of cognate DCs, etc.) collapse onto one consolidated master curve when the fraction of T cells arrested is plotted against this scaling variable. This result demonstrates that since the time required for T cells to traverse the LN is not limiting, antigen quality and quantity determine the time to transition from phase one to phase two via an interplay between the time scales necessary for a productive T-cell-DC encounter ( $\tau_s$ ) and the time scale describing the loss of peptides from DCs ( $\tau$ ). The smaller the value of the ratio of these two time scales ( $\tau/\tau_s$ ), the longer the time required for a transition to take place (or equivalently, the lower the fraction of T cells arrested prior to exit).

Henrickson et al. (22) observed that a twofold decrease in pMHC per DC has more impact on T-cell proliferation than a 10-fold increase in the number of cognate DCs. Our analyses and results suggest that this is because the impact of changes in the numbers of pMHC per DC on  $\tau/\tau_s$  exhibits a threshold, which is because the relationship between the signaling efficiency and the pMHC concentration is not linear, as discussed earlier (Fig. 2). On the other hand, the number of cognate DCs,  $\rho$ , affects this ratio in a linear fashion, as the relationship  $\tau/\tau_s = \rho \int_0^t k(t')dt'$  implies. Therefore, a twofold decrease in the initial pMHC concentration leads to a much greater reduction in  $\rho \int_0^t k(t')dt'$  which can only be compensated by a significantly larger increase in the cognate DC number.

We have also studied situations where there is no antigen loss with time, since peptide half-lives in MHC class II systems can be very long. Furthermore, in some settings, DCs could continuously synthesize new pMHC molecules from an intracellular pathogen or self antigen. In these cases, there is only one relevant time scale,  $\tau_s$ , and it equals  $1/(k \times \rho)$  (note that  $k$ , the probability of receiving a stop signal, does not change with time in this case). Indeed, for these cases, our simulation results obtained from varying the concentration of pMHC ligands or the cognate DC numbers collapse to one consolidated master curve when time is scaled (divided) by  $\tau_s$  (data not shown).

**The need for signal integration.** The fact that the diffusion time is short implies that T cells can efficiently scan many DCs (5, 7, 10, 32, 41) in a period shorter than the time at which the transition from phase one to phase two occurs. Previous studies (e.g., Bousso and Robey [7], Miller et al. [32], and Beltman et al. [5]) show that DCs scan many T cells in a time scale shorter than the duration of phase one. However, the transition from phase-one- to phase-two-type behavior requires 6 to 10 h for 10  $\mu\text{M}$  of the C peptide (22, 30). Given that the time required to encounter a cognate DC is relatively short, why does this transition not occur at earlier times when the antigen dose is higher since fewer peptides have dissociated from DC surfaces? This is likely because the propensity for generating a stop signal is low from the very beginning in these systems. This, in turn, suggests that T cells may be integrating signals from multiple sequential interactions with DCs because of a “memory” that is intrinsic to the topology of the signaling

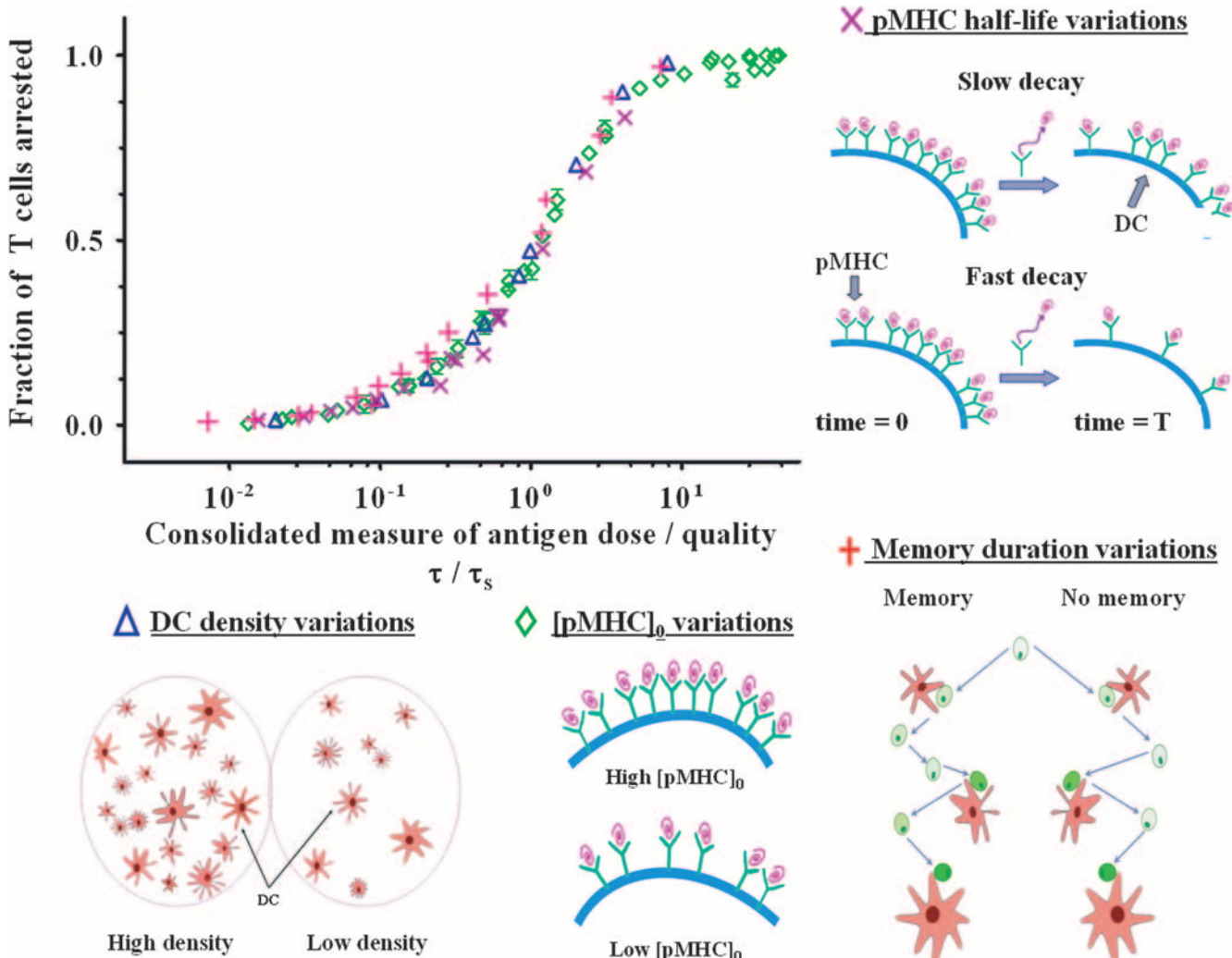


FIG. 4. Unifying conceptual framework describing how antigen dose and quality determine the transition from phase-one- to phase-two-type behavior. Results obtained upon varying diverse quantities (green diamonds, initial pMHC concentration on DCs prior to adoptive transfer and TCR-pMHC binding characteristics; blue triangles, the number of cognate DCs; purple x's, stability of pMHC complexes) all fall on the same consolidated curve when graphed against the consolidated measure of antigen dose/quality. The latter is calculated as the ratio of two time scales, namely the time scale of pMHC loss from the cognate DC surface ( $\tau$ ) and the time scale for a productive T-cell–DC encounter to take place ( $\tau_s$ ) (see the text for derivation). Results of simulations carried out with or without the “memory effect” (the ability to integrate signals from serial T-cell–DC encounters) also fall on the same curve (red crosses). Variations of one parameter and simultaneous variation of two parameters are considered. The number of cognate DCs is varied from 50 to 500; the initial pMHC concentration is varied from 3 to 16,000; the half-life of pMHC is varied from 40 min to 16 h; the memory time scale,  $\tau_m$ , is varied from 0 to 6 h. Increasing the number of DCs, pMHC pulsing concentration, or stability, as well as the memory time scale, all lead to a larger fraction of T cells arrested prior to the exit time (24 h). We also applied modifications to the scheme of T-cell activation upon cognate encounter. Specifically, in alternative scheme 1, instead of being able to receive a stop signal during the entire scanning period (three steps), the T cell can only receive a stop signal during the first waiting step, i.e., immediately after the encounter happens. In the second alternative scheme, the T cell can receive a stop signal throughout the scanning period but peptide loss is allowed during this time, leading to progressively smaller values of  $k$ . We were able to reproduce the master curve for each modified scheme similar to the one shown here.

network. In light of this, we explored the consequences of such a phenomenon in our computer simulations.

**Effects of signal integration.** The T-cell signaling network has many features that could potentially enable signal integration. For example, disassembly of membrane-proximal signaling complexes formed upon interactions with TCR will occur some time after the initial stimulus is removed. Many feedback loops have also been identified in TCR signaling, including those involved in membrane-proximal signaling that may be

relevant for early events that result in a stop signal (1, 36, 49). These feedback loops could potentially provide additional mechanisms for signal integration. Moreover, recent imaging experiments have examined the ability of T cells to integrate signals derived from successive encounters (11, 22, 40), and biochemical experiments have suggested the existence of memory in T-cell signaling (15). Finally, while endogenous pMHC are not explicitly considered in our model, T-cell encounters with DCs displaying endogenous pMHC may also contribute to

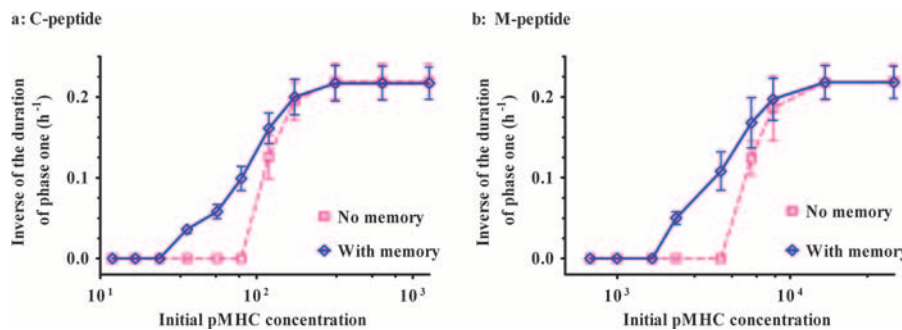


FIG. 5. The ability to integrate signals from serial T-cell–DC encounters lowers the antigen dose required to enable a T cell to transition from phase-one- to phase-two-type behavior. The inverse of the mean duration of phase one is plotted as a function of the initial pMHC concentration on DCs after pulsing prior to adoptive transfer. The duration of phase one is defined as the time required for 50% of the T cells to make sustained contacts with DCs, as described in the text. The way in which signal integration (memory) is incorporated is described in the text. The time scale for memory decay is 160 MC steps (or minutes). (a) The half-life of the pMHC ligand is 2.35 h (corresponds to the C peptide in experiments reported in reference 22). (b) The half-life of the pMHC ligand is 6 h (corresponds to the M peptide in experiments reported in reference 22). For the results in both panels, 100 cognate DCs were simulated. The effects of memory are more pronounced for the less-stable pMHC ligand (a). For example, there is a 58% reduction in the dose required for a transition to phase-two-type behavior in panel a upon incorporation of memory and a 52% reduction in panel b. These specific values depend upon the number of cognate DCs, TCR-pMHC binding characteristics, and other relevant parameters. However, they are almost independent of the time scale characterizing memory (see the text) if this quantity exceeds a threshold value.

a “memory”, since such interactions could help sustain the effects of encounters with cognate ligands.

In future modeling and experimental efforts, molecular details of signaling and migration must be examined simultaneously in order to understand the origin and effects of memory in detail. At present, however, we adopt a minimalist approach by postulating that the T-cell signaling network has a “memory” of previous encounters with DCs, which decays with a characteristic time scale,  $\tau_m$ .  $\tau_m$  is determined by the molecular details of the signaling network, although currently the precise origin and values of this time scale are unknown.

Specifically, we use the following protocol to simulate signal integration from serial T-cell–cognate DC encounters. A “memory”,  $M$  (which initially equals zero), is associated with each T cell. Upon the first T-cell–cognate DC encounter,  $k$  is evaluated using the same procedure as in the case without memory. Should this encounter be unproductive, the T cell leaves with a memory of  $M = k(t)$ , where  $t$  is the time for the first encounter with the cognate DC for this T cell. Prior to the next encounter with a cognate DC at some later time  $t'$ , the memory decays with some time scale,  $\tau_m$ ; thus,  $M(t') = M(t)\exp\{-[(t' - t)/\tau_m]\}$ . At the second cognate DC encounter, the total propensity to receive a stop signal is as follows:  $k_{\text{total}}(t') = k(t') + M(t')$  or 1, whichever is smaller. If the T cell does not receive a stop signal, the value of  $k_{\text{total}}$  is added to its “memory.” In this manner, the “memory,”  $M$ , of previous encounters may enhance the propensity of a stop signal. This process is repeated upon subsequent encounters. Since values of  $\tau_m$  that are significantly shorter than the time scale between successive encounters of a T cell with a cognate DC would have little effect and values comparable to the exit time are unlikely, we focused our studies on values of  $\tau_m$  which are on the order of a diffusion time scale.

Our computer simulations show that initial pMHC concentrations on DCs that would otherwise not result in a transition to phase two may stimulate sustained contacts when signal integration is incorporated (Fig. 5). These results suggest that even if pMHC concentrations on DCs in the LN are so low that

a single T-cell–DC encounter cannot be productive, integration of signals from serial encounters can result in extended T-cell–DC contacts. This concurs with experimental findings by Henrickson et al. (22) which show a transition to phase-two-type behavior under conditions where the antigen density on any particular DC must be quite small. Figure 5 shows that the effects of signal integration are more pronounced for the less stable pMHC ligands (e.g., the C peptide in the work of Henrickson et al.). With the same degree of signal integration (i.e., the same decay rate of the signal;  $\tau_m = 160$  min), the threshold concentration of pMHC required to induce a transition to phase two is reduced by 52% for the M peptide and 58% for the C peptide. This is because given the same initial antigen density loaded onto DCs ex vivo, DCs will display fewer of the less stable pMHC ligands in the LN. The ability to integrate signals from serial encounters therefore becomes more important for the less-stable pMHC antigen. This is also true for the other values of  $\tau_m$  we had examined using computer simulation. With a larger  $\tau_m$  value (more persistent “memory”), the threshold concentration required to induce a transition to phase two can be reduced until a maximum enhancement is reached, beyond which a larger  $\tau_m$  value no longer reduces the threshold concentration (Table 2).

Note, however, that the shapes of the curves in Fig. 5 are not altered by incorporating signal integration. Signal integration simply reduces the time scale required for a productive T-cell–DC encounter ( $\tau_s$ ) if a T cell has previously encountered cognate DCs and in so doing increases the fraction of arrested T cells. In other words, signal integration increases the average probability for a stop signal (i.e., the mean value of  $k$ ) during the process, since the loss of cognate ligands from the DC surface is ameliorated. This makes the effective value of  $\tau/\tau_s$  smaller. Figure 4 makes this point strikingly, since all the simulation results, with and without signal integration, exhibit the same scaling behavior with respect to the interplay of the important time scales identified earlier. As we note in the next section, the same would be true if memory was conferred by

DCs changing pMHC presentation efficiency upon repeated encounters with cognate T cells.

## DISCUSSION

Understanding the behavior of T cells in lymphoid tissue as they begin to be primed by antigen-presenting cells is very important since it is a key stage that leads to the detection of antigen and the mounting of an immune response. Progress in this regard has been aided by the recent application of multiphoton microscopy technology (51, 52) to immunological questions, since this has enabled spatially resolved *in vivo* imaging of T cells in real time (2, 6–8, 11, 23, 30, 32–34, 37, 38, 40, 43, 47). Among the earliest findings from these studies was that the migratory pattern of T cells (on large length and time scales) exhibited the statistical features characteristic of a random walk (32, 34). Subsequent computer simulations have suggested that this enables efficient scanning of DCs in LNs (5). Furthermore, recent experiments suggest that the apparently random (or diffusive) motion may be because T cells follow “tracks” made up of reticular fibers which span the LN in a statistically random manner, and T cells can choose different tracks at the intersections (2, 3). Other important findings are that chemokines can influence the details of T-cell motility patterns (9, 19, 42, 48) and that T cells can organize into dynamic “streams” (5).

The dynamic characteristics of T-cell migration in LNs varies over time (23, 30, 33, 37, 40). In CD8<sup>+</sup> T cells, the first stage (phase one) of rapid scanning (characterized by random walk statistics) is followed by a second phase wherein T cells make extended contacts with DCs. In this second phase, presumably, T cells are making sustained contacts with DCs that are known to be necessary *in vitro* for full commitment to activation (e.g., see reference 24). Therefore, a mechanistic understanding of which factors determine the transition into phase two and how they regulate this decision is crucial. Such an understanding was not available, which was the impetus for this study.

We reasoned that the transition from phase one to phase two results from T-cell signaling stimulated by encounters with cognate DCs. This, in turn, suggested that this transition is strongly influenced by the quantity and quality of antigen. We have studied this hypothesis extensively *in silico* by systematically varying conditions that determine antigen quantity and quality. Our results are qualitatively consistent with experimental observations (22), and they provide a mechanistic framework that describes how antigen dose and type impact the ability of T cells to detect antigen and “decide” to make extended contacts with DCs.

Increasing the initial concentration of cognate ligands loaded on DCs or increasing the fraction of cognate DCs reduces the duration of phase one, because both actions lead to a higher propensity for a productive T-cell–DC encounter. If the antigen concentration on DCs and/or the density of cognate DCs exceeds a threshold value, the transition from phase one to phase two occurs very rapidly. This may explain why it is difficult to observe phase-one-type behavior in a system characterized by high doses of high-affinity antigen on the majority of endogenous LN DCs (38).

Stability of the pMHC complex itself is also an important variable, with more stably bound peptides resulting in a shorter

phase one. This is because unlike the case with *in vitro* experiments with multiple or single cells or lipid bilayers, a T cell might encounter a DC in the LN several hours after antigen loading (as in the experiments reported in references 23, 30, 32 to 34, and 37). During this time, peptides are lost from the DC surfaces. The less stable pMHC complex will thus display smaller amounts of cognate ligand, thereby decreasing the probability of productive T-cell–DC encounters.

The power of our theoretical analysis is that it shows that these seemingly unrelated findings emerge from a single conceptual framework. We have identified three important time scales. The first is the characteristic time for T cells to find DCs bearing cognate ligands, which is rather short for conditions that have been studied previously (7, 23, 32, 41) and by us. Therefore, it is not as important a determinant for the transition from phase-one- to phase-two-type behavior. It is worth remarking, however, that in the early stages of a real infection, the number of DCs bearing a cognate ligand may be smaller than that in *in vivo* imaging experiments (e.g., ~100 to 300 cognate antigen-bearing DCs are in the draining LN at the time of T-cell adoptive transfer in the experiments of Henrickson, et al. [22]), and this time scale may become important. It may also become important if an antigen dose is extremely high, in which case the T cells would receive a sufficiently high stimulus from the first cognate DC they encounter. As a result, the time it takes to encounter the first cognate DC dictates the duration of phase one.

An important time scale is the time required for a productive T-cell–DC encounter to occur ( $\tau_s$ ). Using a mean-field approach, we derived how this time scale is determined by various measures of antigen dose and type. Specifically, we identified the nondimensional ratio of  $\tau_s$  and the half-life of the pMHC complex as the composite variable which controls the behavior of the system. Our simulation results for a wide range of values of diverse quantities that reflect antigen dose and quality all collapse onto one master curve when plotted against this ratio. For systems where antigen loss due to peptide dissociation is not important, diverse results scale with  $\tau_s$  alone since it is the only relevant time scale.

These results show that differences in T-cell migratory patterns observed upon manipulating different variables (antigen dose, density of DCs bearing cognate ligands, peptide stability, TCR-pMHC binding, etc.) result from how this particular change, combined with all other prevailing conditions, affects the  $\tau/\tau_s$  ratio. Changing each of these variables changes the balance between two relevant time scales, thereby influencing the way in which migrating T cells interact with and respond to DCs. We hope that these implications of the conceptual framework revealed by our study will help guide future experimentation.

Our computer simulations and experiments reported by Henrickson et al. (22) both highlight the existence of a sharp threshold in the antigen dose on DCs beyond which the T cell's ability to transition to phase two drastically improves. The value of this threshold concentration is higher for the less stable pMHC ligands and weaker TCR-pMHC binding characteristics (also observed *in vitro* [40]). The existence of a threshold is predicated by the fact that dose-response curves characterizing T-cell signaling exhibit a threshold (29, 44).

The time scale associated with T-cell–DC encounters is

much shorter than the times at which a transition from phase-one- to phase-two-type behavior is observed in the experimental study by Henrickson et al. (22). This observation, combined with the fact that there is a larger amount of pMHC ligands on cognate DCs at shorter times, led us to suggest that T cells may be able to integrate signals from multiple serial encounters with DCs. This aspect of our study differs from previous studies, such as a recent study by Preston et al. (35), in which the detection of antigen and activation of T cells are viewed as a transport-limited process, i.e., the T cells commit to activation upon their first encounter with cognate DCs. Signal integration could result from various aspects of the T-cell signaling network that may confer memory. Our calculations show that such memory effects would enable a transition from phase-one- to phase-two-type behavior when it otherwise may not have occurred because of too low an antigen dose on DCs. We believe that *in vivo*, productive T-cell-cognate DC interactions are stochastic events. The ability to integrate signals from sequential T-cell-DC encounters enhances the sensitivity with which T cells can detect antigen. Furthermore, it may also narrow the distribution of stochastic times at which individual T cells stop, thereby making the transition to phase-two-type behavior appear to be more sharply defined.

It has been suggested that DCs may alter the presentation of pMHC ligands upon serial encounters with T cells, which provides the source of such "memory" (23). In our current model, this would simply result in a different type of variation of the propensity of a productive T-cell-DC encounter ( $k$ ) with time. Thus, it will result in a different value for the ratio of the two important time scales we have identified. Nevertheless, as noted earlier, the results will still depend only on this ratio, and simulations carried out with DCs as the source of memory will also collapse onto the consolidated master curve shown in Fig. 4. Resolving whether the origin of "memory" lies in the T-cell signaling network and/or pMHC presentation on DCs requires the integration of molecular-signaling models with migration simulations and concomitant experiments. It is expected that the details of the temporal migratory patterns should be different in the two cases, since the dynamical behavior of the T-cell signaling network and enhanced pMHC presentation on DCs (e.g., by clustering ligands) should be very different. Experiments aimed toward resolving this have been described by Henrickson et al. (22).

The close connection between T-cell signaling and migration revealed by our studies highlights the need for experimental and computational studies that connect molecular-scale signaling processes to migratory patterns in detail. Multiscale computational models that seamlessly integrate molecular signaling events with T-cell motion are required. Furthermore, the development of efficient computer simulation methods that do not employ a lattice representation of space and can simultaneously incorporate the complexity of signaling is required if all noncognate T cells and DCs are to be included in order to generate models that are quantitatively accurate. Similarly, experimental technologies that can combine the tracking of T-cell motion with the imaging of signaling molecules (as is currently possible *in vitro*) must be developed. Synergy between such experiments and computational studies will help elucidate how T cells are activated in lymphoid tissues.

## ACKNOWLEDGMENTS

Primary support was provided by NIH grant 1 PO1 AI071195-01. Other support to A.K.C. (NIH Director's Pioneer Award), U.H.V.A. (NIH grants RO1 AI069259, AI072252, and AR42689), S.H. (HL07623 and MSTP funding), and A.S.P. (NIH R37 AI28433) is also noted.

Comments from Ira Mazo, Silke Paust, Antonio Peixoto, Fulvia Vascotto, Elisabeth Vollmann, and other members of the von Andrian lab helped improve the clarity of the paper.

## REFERENCES

- Altan-Bonnet, G., and R. N. Germain. 2005. Modeling T cell antigen discrimination based on feedback control of digital ERK responses. *PLoS Biol.* **3**:1925–1938.
- Bajenoff, M., J. G. Egen, L. Y. Koo, J. P. Laugier, F. Brau, N. Glaichenhaus, and R. N. Germain. 2006. Stromal cell networks regulate lymphocyte entry, migration, and territoriality in lymph nodes. *Immunity* **25**:989–1001.
- Beauchemin, C., N. M. Dixit, and A. S. Perelson. 2007. Characterizing T cell movement within lymph nodes in the absence of antigen. *J. Immunol.* **178**: 5505–5512.
- Beltman, J. B., A. F. M. Maree, and R. J. de Boer. 2007. Spatial modelling of brief and long interactions between T cells and dendritic cells. *Immunol. Cell Biol.* **85**:306–314.
- Beltman, J. B., A. F. M. Maree, J. N. Lynch, M. J. Miller, and R. J. de Boer. 2007. Lymph node topology dictates T cell migration behavior. *J. Exp. Med.* **204**:771–780.
- Bousso, P., N. R. Bhakta, R. S. Lewis, and E. Robey. 2002. Dynamics of thymocyte-stromal cell interactions visualized by two-photon microscopy. *Science* **296**:1876–1880.
- Bousso, P., and E. Robey. 2003. Dynamics of CD8(+) T cell priming by dendritic cells in intact lymph nodes. *Nat. Immunol.* **4**:579–585.
- Bousso, P., and E. A. Robey. 2004. Dynamic behavior of T cells and thymocytes in lymphoid organs as revealed by two-photon microscopy. *Immunity* **21**:349–355.
- Castellino, F., A. Y. Huang, G. Altan-Bonnet, S. Stoll, C. Scheinecker, and R. N. Germain. 2006. Chemokines enhance immunity by guiding naïve CD8+ T cells to sites of CD4+ T cell-dendritic cell interaction. *Nature* **440**:890–895.
- Catron, D. M., A. A. Itano, K. A. Pape, D. L. Mueller, and M. K. Jenkins. 2004. Visualizing the first 50 hr of the primary immune response to a soluble antigen. *Immunity* **21**:341–347.
- Celli, S., Z. Garcia, and P. Bousso. 2005. CD4 T cells integrate signals delivered during successive DC encounters *in vivo*. *J. Exp. Med.* **202**:1271–1278.
- Cemerski, S., J. Das, J. Locasale, P. Arnold, E. Giurisato, M. A. Markiewicz, D. Fremont, P. M. Allen, A. K. Chakraborty, and A. S. Shaw. 2007. The stimulatory potency of T cell antigens is influenced by the formation of the immunological synapse. *Immunity* **26**:345–355.
- de Gennes, P.-G. 1985. Scaling concepts in polymer physics, 2nd ed. Cornell University Press, Ithaca, NY.
- Dustin, M. L., S. K. Bromley, Z. Y. Kan, D. A. Peterson, and E. R. Unanue. 1997. Antigen receptor engagement delivers a stop signal to migrating T lymphocytes. *Proc. Natl. Acad. Sci. USA* **94**:3909–3913.
- Faroudi, M., R. Zaru, P. Paulet, S. Muller, and S. Valitutti. 2003. Cutting edge: T lymphocyte activation by repeated immunological synapse formation and intermittent signaling. *J. Immunol.* **171**:1128–1132.
- Freed, K. F. 1987. Renormalization group theory of macromolecules. J. Wiley, New York, NY.
- Frenkel, D., and B. Smit. 2001. Understanding molecular simulation. Academic Press, Inc., Orlando, FL.
- Goldstein, B., J. R. Faeder, and W. S. Hlavacek. 2004. Mathematical and computational models of immune-receptor signalling. *Nat. Rev. Immunol.* **4**:445–456.
- Guarda, G., M. Hons, S. F. Soriano, A. Y. Huang, R. Polley, A. Martin-Fonterea, J. V. Stein, R. N. Germain, A. Lanzavecchia, and F. Sallusto. 2007. L-selectin-negative CCR7-effector and memory CD8+ T cells enter reactive lymph nodes and kill dendritic cells. *Nat. Immunol.* **8**:743–752.
- Gunzer, M., A. Schafer, S. Borgmann, S. Grabbe, K. S. Zanker, E. B. Brocker, E. Kampgen, and P. Friedl. 2000. Antigen presentation in extracellular matrix: interactions of T cells with dendritic cells are dynamic, short lived, and sequential. *Immunity* **13**:323–332.
- Halin, C., M. L. Scimone, R. Bonasio, J.-M. Gauguet, T. R. Memel, E. Quackenbush, R. L. Proia, S. Mandala, and U. H. von Andrian. 2005. The SIP-analog FTY720 differentially modulates T-cell homing via HEV: T-cell-expressed SIP1 amplifies integrin activation in peripheral lymph nodes but not in Peyer patches. *Blood* **106**:1314–1322.
- Henrickson, S. E., T. R. Memel, I. B. Mazo, B. Liu, M. N. Artyomov, H. Zheng, A. Peixoto, M. P. Flynn, B. Senman, T. Junt, H. C. Wong, A. K. Chakraborty, and U. H. von Andrian. 2008. T cell sensing of antigen dose

- governs interactive behavior with dendritic cells and sets a threshold for T cell activation. *Nat. Immunol.* **9**:282–291.
23. Hugues, S., L. Fetler, L. Bonifaz, J. Helft, F. Amblard, and S. Amigorena. 2004. Distinct T cell dynamics in lymph nodes during the induction of tolerance and immunity. *Nat. Immunol.* **5**:1235–1242.
  24. Huppa, J. B., M. Gleimer, C. Sumen, and M. M. Davis. 2003. Continuous T cell receptor signaling required for synapse maintenance and full effector potential. *Nat. Immunol.* **4**:749–755.
  25. Kaech, S. M., and R. Ahmed. 2001. Memory CD8+ T cell differentiation: initial antigen encounter triggers a developmental program in naive cells. *Nat. Immunol.* **2**:415–422.
  26. Kayser, R. F., and J. B. Hubbard. 1983. Diffusion in a medium with a random distribution of static traps. *Phys. Rev. Lett.* **51**:79–82.
  27. Kayser, R. F., and J. B. Hubbard. 1984. Reaction diffusion in a medium containing a random distribution of nonoverlapping traps. *J. Chem. Phys.* **80**:1127–1130.
  28. Lee, K. H., A. R. Dinner, C. Tu, G. Campi, S. Raychaudhuri, R. Varma, T. N. Sims, W. R. Burack, H. Wu, O. Kanagawa, M. Markiewicz, P. M. Allen, M. L. Dustin, A. K. Chakraborty, and A. S. Shaw. 2003. The immunological synapse balances T cell receptor signaling and degradation. *Science* **302**:1218–1222.
  29. Li, Q. J., A. R. Dinner, S. Y. Qi, D. J. Irvine, J. B. Huppa, M. M. Davis, and A. K. Chakraborty. 2004. CD4 enhances T cell sensitivity to antigen by coordinating Lck accumulation at the immunological synapse. *Nat. Immunol.* **5**:791–799.
  30. Mempel, T. R., S. E. Henrickson, and U. H. von Andrian. 2004. T-cell priming by dendritic cells in lymph nodes occurs in three distinct phases. *Nature* **427**:154–159.
  31. Mercado, R., S. Vijh, S. E. Allen, K. Kerksiek, I. M. Pilip, and E. G. Palmer. 2000. Early programming of T cell populations responding to bacterial infection. *J. Immunol.* **165**:6833–6839.
  32. Miller, M. J., A. S. Hejazi, S. H. Wei, M. D. Cahalan, and I. Parker. 2004. T cell repertoire scanning is promoted by dynamic dendritic cell behavior and random T cell motility in the lymph node. *Proc. Natl. Acad. Sci. USA* **101**:998–1003.
  33. Miller, M. J., O. Safrina, I. Parker, and M. D. Cahalan. 2004. Imaging the single cell dynamics of CD4(+) T cell activation by dendritic cells in lymph nodes. *J. Exp. Med.* **200**:847–856.
  34. Miller, M. J., S. H. Wei, I. Parker, and M. D. Cahalan. 2002. Two-photon imaging of lymphocyte motility and antigen response in intact lymph node. *Science* **296**:1869–1873.
  35. Preston, S. P., S. L. Waters, O. E. Jensen, P. R. Heaton, and D. I. Pritchard. 2006. T-cell motility in the early stages of the immune response modeled as a random walk amongst targets. *Phys. Rev. E* **74**:011910.
  36. Reth, M., and T. Brummer. 2004. Feedback regulation of lymphocyte signalling. *Nat. Rev. Immunol.* **4**:269–277.
  37. Schneider, H., J. Downey, A. Smith, B. H. Zinselmeyer, C. Rush, J. M. Brewer, B. Wei, N. Hogg, P. Garside, and C. E. Rudd. 2006. Reversal of the TCR stop signal by CTLA-4. *Science* **313**:1972–1975.
  38. Shakhar, G., R. L. Lindquist, D. Skokos, D. Dudziak, J. H. Huang, M. C. Nusseznweig, and M. L. Dustin. 2005. Stable T cell-dendritic cell interactions precede the development of both tolerance and immunity in vivo. *Nat. Immunol.* **6**:707–714.
  39. Shiow, L. R., D. B. Rosen, N. Brdickova, Y. Xu, J. P. An, L. L. Lanier, J. G. Cyster, and M. Matloubian. 2006. CD69 acts downstream of interferon-alpha/beta to inhibit SIP1(1) and lymphocyte egress from lymphoid organs. *Nature* **440**:540–544.
  40. Skokos, D., G. Shakhar, R. Varma, J. C. Waite, T. O. Cameron, R. L. Lindquist, T. Schwickert, M. C. Nusseznweig, and M. L. Dustin. 2007. Peptide-MHC potency governs dynamic interactions between T cells and dendritic cells in lymph nodes. *Nat. Immunol.* **8**:835–844.
  41. Slifka, M. K., R. Antia, J. K. Whitmire, and R. Ahmed. 1998. Humoral immunity due to long-lived plasma cells. *Immunity* **8**:363–372.
  42. Stachowiak, A. N., Y. Wang, Y. C. Huang, and D. J. Irvine. 2006. Homeostatic lymphoid chemokines synergize with adhesion ligands to trigger T and B lymphocyte chemokinesis. *J. Immunol.* **177**:2340–2348.
  43. Stoll, S., J. Delon, T. M. Brotz, and R. N. Germain. 2002. Dynamic imaging of T cell-dendritic cell interactions in lymph nodes. *Science* **296**:1873–1876.
  44. Sykulev, Y., A. Brummark, M. Jackson, R. J. Cohen, P. A. Peterson, and H. N. Eisen. 1994. Kinetics and affinity of reactions between an antigen-specific T cell receptor and peptide-MHC complexes. *Immunity* **1**:15–22.
  45. van Stipdonk, M. J. B., G. Hardenberg, M. S. Bijk, E. E. Lemmens, N. M. Droin, D. R. Green, and S. P. Schoenberger. 2003. Dynamic programming of CD8+ T lymphocyte responses. *Nat. Immunol.* **4**:361–365.
  46. van Stipdonk, M. J. B., E. E. Lemmens, and S. P. Schoenberger. 2001. Naive CTLs require a single brief period of antigenic stimulation for clonal expansion and differentiation. *Nat. Immunol.* **2**:423–429.
  47. Wei, S. H., O. Safrina, Y. Yu, K. R. Garrod, M. D. Cahalan, and I. Parker. 2007. Ca2+ signals in CD4+ T cells during early contacts with antigen-bearing dendritic cells in lymph node. *J. Immunol.* **179**:1586–1594.
  48. Worbs, T., T. R. Mempel, J. Bolter, U. H. von Andrian, and R. Förster. 2007. CCR7 ligands stimulate the intranodal motility of T lymphocytes in vivo. *J. Exp. Med.* **204**:489–495.
  49. Wylie, D. C., J. Das, and A. K. Chakraborty. 2007. Sensitivity of T cells to antigen and antagonism emerges from differential regulation of the same molecular signaling module. *Proc. Natl. Acad. Sci. USA* **104**:5533–5538.
  50. Young, A. J. 1999. The physiology of lymphocyte migration through the single lymph node in vivo. *Semin. Immunol.* **11**:73–83.
  51. Zipfel, W. R., R. M. Williams, R. Christie, A. Y. Nikitin, B. T. Hyman, and W. W. Webb. 2003. Live tissue intrinsic emission microscopy using multiphoton-excited native fluorescence and second harmonic generation. *Proc. Natl. Acad. Sci. USA* **100**:7075–7080.
  52. Zipfel, W. R., R. M. Williams, and W. W. Webb. 2003. Nonlinear magic: multiphoton microscopy in the biosciences. *Nat. Biotechnol.* **21**:1368–1376.